Lattice Site Location Studies of Rare-Earths Implanted in ZnO Single-Crystals

Elisabete M.C. Rita [1,2], Ulrich Wahl [1,2], Armandina L. Lopes [3], João P. Araújo [4],
João G. Correia [1,2,5], Eduardo Alves [1,2], José C. Soares [1,2], and the ISOLDE Collaboration [5]
[1] Instituto Tecnológico e Nuclear, Estrada Nacional 10, PT-2685 Sacavém, Portugal
[2] CFNUL, Av. Prof. Gama Pinto 2, PT-1699 Lisboa Codex, Portugal
[3] Departamento de Física da Universidade de Aveiro, PT-3800 Aveiro, Portugal
[4] IFIMUP, University of Porto, PT-4150 Porto, Portugal
[5] CERN-EP, CH-1211 Geneva 23, Switzerland

ABSTRACT

In this work we report on the lattice site location of rare earths in single-crystalline ZnO by means of the emission channeling (EC) technique. Following low dose (3×10^{13}at/cm^2) 60 keV ion implantation of the precursor isotope ^{169}Yb, a position-sensitive electron detector was used to monitor the angular distribution of the conversion electrons emitted from ^{169}Tm* as a function of the annealing temperature up to 600°C in vacuum. An additional annealing at 800°C in flowing O$_2$ was performed. The EC measurements revealed that around 95-100% of the rare earth atoms occupy substitutional Zn sites up to an annealing temperature of 600°C/vacuum. After the 800°C/O$_2$ annealing, the emission channeling effects decreased considerably.

INTRODUCTION

Rare earth doped semiconductors exhibit visible or infrared luminescence and are of interest for optoelectronic applications, for instance, as light emitting diodes [1]. Experimental evidence of high luminescence efficiency from rare earths in wide band gap semiconductors [2], such as GaN, pointed out these systems as possible materials for electroluminescent devices. The II-VI compound zinc oxide (ZnO) is one of the materials investigated in that respect. With a band gap of similar width as GaN, this oxide offers the advantage of growing high quality bulk single crystals more easily.

Rare earth doping of ZnO during growth has already been described previously in the literature [3-10]. However, the production of doped layers by ion implantation, the main doping technique used in semiconductor technology, has not been exploited to a great extent. A fundamental step to understand the doping effects from implanted elements is to learn their lattice location. In the particular case of low concentrations of implanted elements, this can be achieved using the emission channeling (EC) technique, which makes use of the fact that charged particles emitted from radioactive isotopes in single-crystals experience channeling or blocking effects along crystallographic axis and planes.

In this work we report on the lattice location of the rare earth isotope ^{169}Tm* ($t_{1/2}$=0.66 μs) in a ZnO single crystal using emission channeling, following ion implantation of its precursor ^{169}Yb ($t_{1/2}$=32 d). The ^{169}Yb probe nuclei decay by electron capture to the excited state ^{169}Tm*, which decays to the ^{169}Tm ground state. The latter transition is accompanied by conversion electron emission, which can be used for EC [11]. Using position-sensitive electron detectors [11] the angular distribution of the conversion electrons is measured and provides information about the emitter (^{169}Tm*) lattice site. Note that since the recoil energy in the ^{169}Yb $\rightarrow$ ^{169}Tm* nuclear decay is less than 1.1 eV, it is most likely that ^{169}Tm* has inherited the ^{169}Yb lattice site [11].

EXPERIMENT

In this study a commercially available ZnO [0001] single-crystal [12], grown by seeded chemical vapor transport and polished on the O face, was implanted at room temperature with the radioactive isotope ^{169}Yb up to a dose of $3{\times}10^{13}$ at/cm^2 and 60 keV energy. This was performed at the CERN/ISOLDE facility [13], where pure beams of radioactive elements are produced, providing a large variety of isotopes for EC. In order to minimize the fraction of ^{169}Yb atoms channeled during implantation and provide a well-defined depth profile, a 7° tilt angle from the crystal surface was applied. The resulting range, straggling and peak concentration of ^{169}Yb atoms, as estimated from TRIM calculations [14], are 166 Å, 54 Å, and $2{\times}10^{19}$ cm^{-3}, respectively.

The emission channeling patterns of the conversion electrons emitted as a consequence of the ^{169}Yb decay were recorded in vacuum with the position-sensitive detection system described in Ref. [11]. Setting an energy window above 95 keV included the 100, 109, 118, 121, 139, 188, 248 and 298 keV conversion electrons emitted by the ^{169}Tm* ($t_{1/2}$=0.66 µs) state but excluded lower energy electrons from short-lived states which are populated within a few ns following the ^{169}Yb decay. The angular distributions were measured around the [0001], [$\bar{1}1102$], [$\bar{1}101$] and [$\bar{2}113$] directions of the ZnO crystal in the as-implanted state and after 10 min *in situ* vacuum annealing at 300°C and 600°C, and *ex situ* annealing at 800°C in flowing O$_2$.

The subsequent evaluation of the Tm sites in the ZnO lattice was achieved by fitting the experimental channeling patterns with simulated ones. The ^{169}Tm* theoretical emission channeling patterns were calculated by means of the "many beam" theory of electron diffraction in single-crystals [15]. To describe the ZnO crystal structure we applied the following structural model. We used lattice constants of $a = 3.2495$ Å and $c = 5.2069$ Å [16] and assumed the Zn-O c-axis bond length to be $z = 0.375\ c$, as in an ideal wurtzite structure. In addition, isotropic root mean square (rms) displacements of u_1(Zn) = 0.082 Å and u_1(O) = 0.085 Å [17] were applied, which would correspond to Debye temperatures of T_D(Zn) = 320 K and T_D(O) = 696 K. In the simulations, the angular range of 0°-3° around each of the investigated crystal directions was considered in small steps of $\Delta x = \Delta y = 0.05°$. In order to quantitatively compare experimental and theoretical patterns, the two-dimensional fitting procedure outlined in Ref. [11] was used. The considered lattice sites were substitutional Zn sites (S_{Zn}) and substitutional O sites (S_O) with varying root mean square (rms) displacements and a variety of interstitial sites, which are described in detail in Ref. [18].

RESULTS

The experimental emission channeling pattern for the [0001] direction following the 300°C annealing step in vacuum is shown in Fig. 1 (a). The observed channeling effect gives direct evidence of the presence of ^{169}Tm* atoms along the c-axis. The best two-fraction fit of the theoretical yields to the experimental data is represented in Fig. 1 (e) and corresponds to 104% of Tm atoms along the c-axis. The Tm rms displacement from the c-axis which gave the best fit was 0.12 Å (note that the channeling effect is not sensitive to displacements along the channeling direction). The fitted Tm fraction somewhat exceeds 100% but this is well within the expected accuracy. For instance, the absolute comparison between experiment and theory requires the measured patterns to be corrected for the influence of backscattered electrons. The typical errors in-

troduced by this procedure can be around ~10%, and since the correction factors also depend on the angle between sample normal and detector, not all patterns are influenced in the same way.

We would like to point out that all sites located along the c-axis would cause an emission channeling pattern similar to the one shown in Fig. 1 (a), among them, for instance, substitutional S_{Zn} and S_O or interstitial T sites. Therefore, to achieve an unambiguous lattice site location, the information obtained along the $[\bar{1}1102]$, $[\bar{1}101]$ and $[\bar{2}113]$ directions was considered as well. The experimental patterns for these directions are shown in Figs. 1 (b), (c) and (d), respectively, for the same 300°C annealing step. For each of them good fits to the experimental yields were achieved considering only two fractions for the Tm atoms, namely, substitutional at Zn sites S_{Zn}, and at random sites, which are supposed to produce an isotropic emission yield. The best two-fraction fits are displayed in Figs. 1 (f), (g) and (h).
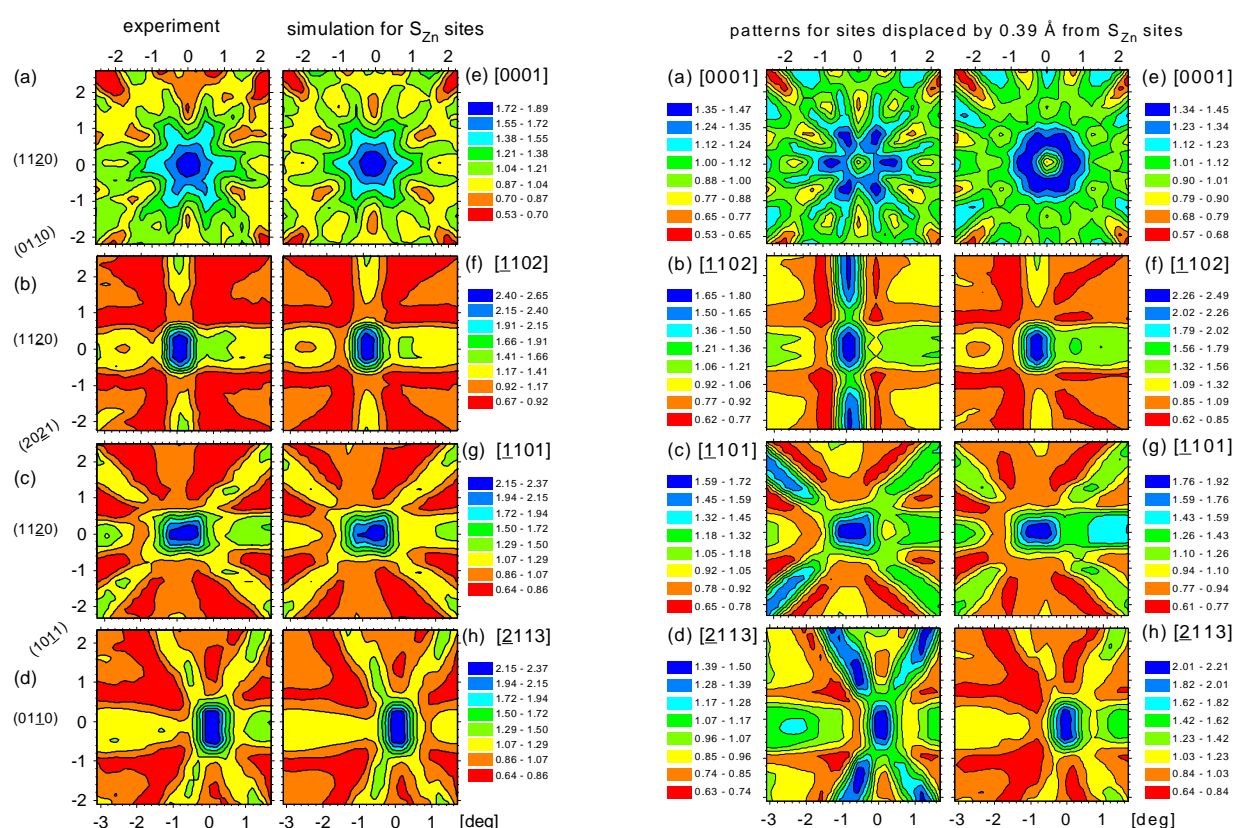

Figure 1. Angular distributions of the $^{169}Tm^*$ conversion electron yields around the [0001] (a), $[\bar{1}1102]$ (b), $[\bar{1}101]$ (c) and $[\bar{2}113]$ (d) directions following the 300°C vacuum annealing. The best fits of the channeling patterns for each direction are also shown and correspond to 104% (e), 96% (f), 104% (g) and 89% (h) of Tm atoms at S_{Zn} sites with rms displacements of 0.12 Å, 0.12 Å, 0.16 Å and 0.15 Å, respectively.

Figure 2. Examples for best fits due to sites which are displaced by 0.39 Å from substitutional Zn sites, corresponding to 4/10 of the distance towards anti-bonding (AB) or bond center (BC) sites. (a)-(d) are patterns for displacements towards AB sites off the c-axis, while the [0001] pattern (e) is for displacements towards BC sites off the c-axis, and the $[\bar{1}102]$, $[\bar{1}101]$ and $[\bar{2}113]$ patterns (f)-(h) are for displacements to AB sites within the c-axis.

Emission channeling patterns are quite sensitive to displacements of the emitter atoms from ideal substitutional sites. In order to illustrate this, we have displayed in Fig. 2 the fits for patterns resulting from emitter atoms that are displaced by 0.39 Å from ideal Zn sites towards interstitial sites. Such a displacement already changes the patterns significantly, resulting in chi square of fit values twice larger than those of the fits shown in Fig. 1. We have also tried to fit the experimental patterns by emitter atoms on S_{Zn} sites plus additional fractions on substitutional O or well-defined interstitial sites. However, the chi square of fit did not improve significantly and possible fractions are below 5%. Note that channeling patterns due to emitter atoms on substitutional O sites S_O or prominent interstitial sites such as H, O_i or T are distinctively different from those of S_{Zn} sites, as we have shown previously [18-20].

The average fraction of Tm atoms at S_{Zn} sites as a function of the annealing temperature is shown in Fig. 3 (a). We stress that the 800°C annealing was performed in flowing O_2, while the previous annealings at lower temperatures were in vacuum. As can be seen, annealing the ZnO single-crystal up to 600°C in vacuum did not result in a considerable change of the Tm fraction at S_{Zn} sites. The same is not valid for the 800°C annealing in flowing O_2, after which this fraction decreased from 96% to 75%.

The room temperature rms displacements of Tm atoms from the perfect S_{Zn} sites, perpendicular to the four investigated directions, and observed following the different annealing steps, are displayed in Fig. 3 (b). For all directions, the Tm rms displacements decreased with increasing annealing temperature up to 600°C vacuum annealing and increased again after 800°C in O_2. Also, the Tm rms displacements are generally higher than the vibrations of Zn and O atoms. However, following the 600°C vacuum annealing the Tm rms displacements reached values close to the lattice vibrations.
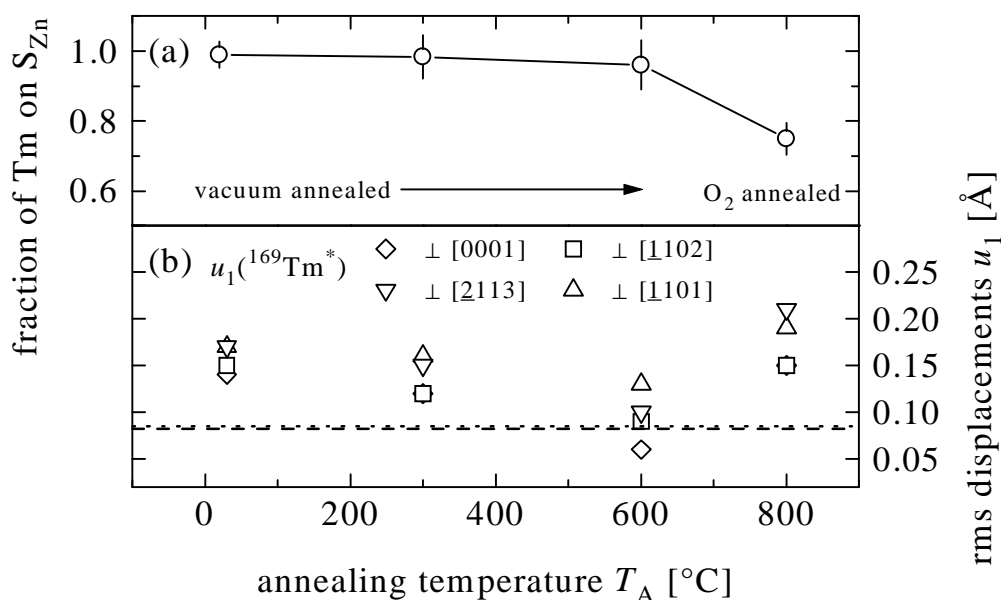
Figure 3. Fraction of Tm atoms at S_{Zn} sites (a) and their rms displacements perpendicular to the [0001], [$\bar{1}$1102], [$\bar{1}$101] and [$\bar{2}$113] directions (b) following 10 min annealing steps (in vacuum up to 600°C and in flowing O_2 at 800°C). The dashed and dotted lines represent the room temperature Zn and O vibration amplitudes, respectively.

DISCUSSION

The recoil energy of the ^{169}Yb $\rightarrow$ ^{169}Tm* nuclear decay is less than 1.1 eV, indicating that the ^{169}Tm* lattice site most probably was inherited from ^{169}Yb. Our emission channeling data thus show that already in the as-implanted state around 95-100% of the rare earth atoms occupy substitutional Zn sites. The fact that no annealing is needed in order to incorporate the rare earths on substitutional sites is a consequence of both the relatively low dose used in our experiment (3×10^{13}at/cm^2) and the high resistance of ZnO against the formation of structural defects by irradiation. However, the slight decrease in the Tm rms displacement as a function of annealing temperature up to 600°C indicates a more perfect incorporation into substitutional Zn sites. This may be explained by the annealing of some structural defects in the neighborhood of the rare earth atoms and is in fact the only indication of defect annealing we have observed in this experiment.

While annealing in vacuum up to 600°C did not change the substitutional Tm fraction, a decrease was observed after the 800°C/O$_2$ annealing step, accompanied by an increase of the Tm rms displacement. In principle this behavior could be due, e.g., to a degradation of the ZnO single-crystal surface during the annealing, which would also introduce disorder in the lattice. However, according to previous experiments which we performed in ZnO single-crystals implanted with Er at the higher dose of 5×10^{15}at/cm^2 [21], a more likely explanation is the diffusion of the rare earth element itself. In this previous study, Rutherford backscattering (RBS) showed nearly complete damage recovery and no surface degradation after 1050°C annealing in air, while only 50% of the implanted Er atoms remained in the crystal following this procedure and the onset of Er diffusion was already visible following 800°C annealing in air.

It is also interesting to compare the present work to our previous emission channeling studies of the lattice location of rare earth ^{167}Tm/^{167m}Er in ZnO [20]. A similar behavior was found in terms of lattice site preference, fractions and rms displacements. In fact, up to 700°C vacuum annealing 75-90% of ^{167m}Er atoms were stable at the S_{Zn} site and a slight decrease in the Er rms displacement was observed [20]. Also, the 800°C annealing step resulted in a decrease of the substitutional Er fraction and an rms displacement increase. Thus the fact that the 800°C vacuum annealing step in the previous Tm/Er experiment was replaced by 800°C annealing under flowing O$_2$ in the present Yb/Tm study, did not significantly change the experimental outcome.

CONCLUSIONS

Our emission channeling experiments show that the majority of Tm atoms (95-100%) are incorporated on substitutional Zn sites following low dose ion implantation at room temperature. We found no evidence for the presence of Tm atoms in other highly symmetric sites than substitutional Zn sites. Annealing the sample up to 600°C in vacuum did not affect the substitutional Tm fraction, but after the 800°C annealing in O$_2$ a considerable decrease of this fraction to 75% was observed, most likely related to rare earth diffusion. With respect to the rare earth doping of ZnO by means of ion implantation, the substitutional incorporation of the rare earth atoms seems hence to be a minor problem, while their diffusion poses a severe limit on the subsequent processing temperatures. This may present problems since the restoration of the optical properties of ZnO following implantation and the optical activation of rare earth dopants generally require annealing at high temperatures [21].

ACKNOWLEDGMENTS

REFERENCES

1. T. Gregorkiewicz and J.M. Langer, *Mat. Res. Soc. Bull*. **24/9**, 27 (1999).
2. P.N. Favennec, H. L'Haridon, D. Moutonnet, M. Salvi, and M. Gauneau, *Mater. Res. Soc. Symp. Proc.* **301**, 181 (1993).
3. V.X. Quang, N.Q. Liem, N.C. Thanh, T.V. Chuong, and L.T. Le Thanh, *Phys. Stat. Sol.* **78**, K161 (1983).
4. S. Bachir, K.Azuma, J. Kossanyi, P. Valat, and J.C. Ronfard-Haret, *J. Lumin.* **75**, 35 (1997).
5. Y.K. Park, J.I. Han, M.G. Kwak, H. Yang, S.H. Ju, and W.S. Cho, *Appl. Phys. Lett.* **72**, 668 (1998).
6. N. Mais, J.P. Reithmaier, A. Forchel, M. Kohls, L. Spanhel, and G. Müller, *Appl. Phys. Lett.* **75**, 2005 (1999).
7. S. Komuro, T. Katsumata, T. Morikawa, X. Zhao, H. Isshiki, and Y. Aoyagi, *Appl. Phys. Lett.* **76**, 3935 (2000).
8. S. Komuro, T. Katsumata, T. Morikawa, X. Zhao, H. Isshiki, and Y. Aoyagi, *J. Appl. Phys.* **88**, 7129 (2000).
9. X. Zhao, S. Komuro, Y. Aoyagi, and T. Sugano, *J. Lumin.* **87-89**, 1254 (2000).
10. S.M. Liu, F.Q. Liu, and Z.G. Wang, *Chem. Phys. Lett.* **343**, 489 (2001).
11. U. Wahl, J.G. Correia, S. Cardoso, J.G. Marques, A. Vantomme, G. Langouche, and the ISOLDE collaboration, *Nucl. Instrum. Meth.* B **136-138**, 744-750 (1998).
12. Purchased from Eagle-Picher Technologies, Miami, OK 74354.
13. E. Kugler, D. Fiander, B. Jonson, H. Haas, A. Przewloka, H. L. Ravn, D. J. Simon, K. Zimmer, and the ISOLDE collaboration, *Nucl. Instrum. Meth. Phys. Res.* B **70**, 41 (1992).
14. J.F. Ziegler and J.P. Biersack, *The Stopping and Range of Ions in Matter* (Pergamon Press, New York, 1985).
15. H. Hofsäss and G. Lindner, *Phys. Rep.* **210**, 121 (1991).
16. U. Rössler, in *Landolt-Börnstein New Series*, Vol. 22, edited by O. Madelung (Springer, Berlin, 1989), p. 163.
17. H. Schulz and K.H. Thiemann, *Solid State Comm.* **32**, 783 (1979).
18. U. Wahl, A. Vantomme, G. Langouche, J.P. Araújo, J.G. Correia, L. Peralta, and the ISOLDE collaboration, *J. Appl. Phys.* **88**, 1319 (2000).
19. U. Wahl, A. Vantomme, G. Langouche, J.G. Correia, L. Peralta, and the ISOLDE collaboration, *Appl. Phys. Lett.* **78**, 3217 (2001).
20. U. Wahl, E. Rita, J.G. Correia, E. Alves, J.P. Araújo and the ISOLDE collaboration, *Appl. Phys. Lett.* (in press).
21. E. Alves, E. Rita, U. Wahl, J.G. Correia, T. Monteiro, and C. Boemare, *Nucl. Instrum. Meth. Phys. Res.* B (in press).